FEMS Microbes, 2024, 5, xtae022
DOI: 10.1093/femsmc/xtae022
Advance access publication date: 26 July 2024
Research Article – Microbes & Disease

Enterococcal quorum-controlled protease alters phage infection

Emma K. Sheriff[1], Fernanda Salvato[2], Shelby E. Andersen[1], Anushila Chatterjee[1], Manuel Kleiner[2], Breck A. Duerkop[1,*]

[1]Department of Immunology and Microbiology, School of Medicine, University of Colorado – Anschutz Medical Campus, 12800 E. 19th Ave., Aurora, CO 80045, United States
[2]Department of Plant and Microbial Biology, North Carolina State University, 112 Derieux Pl., Raleigh, NC 27695, United States
*Corresponding author. Department of Immunology and Microbiology, School of Medicine, University of Colorado - Anschutz Medical Campus, 12800 E. 19th Ave., Aurora, CO 80045, United States. Email: breck.duerkop@cuanschutz.edu
Editor: [Kimberly A. Kline]

Abstract

Increased prevalence of multidrug-resistant bacterial infections has sparked interest in alternative antimicrobials, including bacteriophages (phages). Limited understanding of the phage infection process hampers our ability to utilize phages to their full therapeutic potential. To understand phage infection dynamics, we performed proteomics on *Enterococcus faecalis* infected with the phage VPE25. We discovered that numerous uncharacterized phage proteins are produced during phage infection of *E. faecalis*. Additionally, we identified hundreds of changes in bacterial protein abundances during infection. One such protein, enterococcal gelatinase (GelE), an *fsr* quorum-sensing-regulated protease involved in biofilm formation and virulence, was reduced during VPE25 infection. Plaque assays showed that mutation of either the quorum-sensing regulator *fsrA* or *gelE* resulted in plaques with a "halo" morphology and significantly larger diameters, suggesting decreased protection from phage infection. GelE-associated protection during phage infection is dependent on the putative murein hydrolase regulator LrgA and antiholin-like protein LrgB, whose expression have been shown to be regulated by GelE. Our work may be leveraged in the development of phage therapies that can modulate the production of GelE thereby altering biofilm formation and decreasing *E. faecalis* virulence.

Keywords: *Enterococcus*; bacteriophage; quorum sensing; protease; proteomics; phage–host interactions

Introduction

Enterococcus faecalis is a Gram-positive bacterium and a member of the gut microbiota of diverse animals, including humans (Sghir et al. 2000, Eckburg et al. 2005, Hayashi et al. 2005). Following prolonged antibiotic therapy, *E. faecalis* can outgrow other members of the microbiota and disseminate to the bloodstream, leading to life threatening diseases such as sepsis and endocarditis (Agudelo Higuita and Huycke 2014, Holland et al. 2016, Vogkou et al. 2016, Østergaard et al. 2022). Additionally, *E. faecalis* is a common cause of healthcare-associated infections (Huycke et al. 1998, Giacometti et al. 2000, Lake et al. 2018). Treatment of enterococcal infections is complicated by the increasing prevalence of multidrug-resistant (MDR) strains, including those resistant to "last-resort" antibiotics (Van Tyne and Gilmore 2014, Rice et al. 2018, Tyson et al. 2018, García-Solache and Rice 2019). With the ongoing antibiotic discovery gap and rising incidence of MDR infections, it is estimated that over 10 million individuals may die of antibiotic resistant infections per year by 2050, nearly 10 times the current yearly mortality (O'Neill 2016, Murray et al. 2022). Therefore, the development of innovative antimicrobial therapies is crucial to combating antibiotic resistant bacteria.

Bacteriophages (phages) are viruses that infect and kill bacteria. They have reemerged as potential therapeutics due to their diversity and abundance in nature, making them readily available for medical applications (Wigington et al. 2016, Williamson et al. 2017). Despite the discovery of phages over 100 years ago, we know little about the function of most phage-encoded genes (Twort 1915, D'Herelle 1917). Additionally, we have only a rudimentary understanding of how phages interact with their target bacteria, particularly in nonmodel hosts (Hatfull and Hendrix 2011). Understanding these fundamental aspects of phage biology is an important milestone toward the development of phages as antimicrobials.

During infection, phages co-opt host cellular processes to support their genome replication and translation of proteins responsible for virion assembly (Sergueev et al. 2002, Datta et al. 2005). One way that phages influence the bacterial response to infection is by modulating the cell density-dependent transcriptional program known as quorum sensing (QS) (Rossmann et al. 2015, Ali et al. 2017, Schroven et al. 2023, Schwartzkopf et al. 2024). Phage-mediated changes in QS gene regulation within a bacterial population can create an environment that is more permissible for infection (Schroven et al. 2023, Schwartzkopf et al. 2024). For example, changes in QS can result in the modification of wall teichoic acids, a major phage receptor, which contributes to phage infectivity (De Smet et al. 2016, Yang et al. 2023). In *E. faecalis*, high levels of the QS peptide AI-2 are associated with release of prophages, possibly resulting in the transfer of virulence genes (Rossmann et al. 2015). Additionally, *E. faecalis* QS itself is interrupted during phage infection, with decreased transcription of QS-induced genes and increased transcription of QS-repressed genes (Chatterjee et al. 2020).

QS in *E. faecalis* is controlled by the Fsr system (Qin et al. 2001, Ali et al. 2017). This system positively and negatively regulates

Received 5 May 2024; **revised** 21 June 2024; **accepted** 25 July 2024

the expression of hundreds of genes in response to bacterial density, as sensed by the extracellular abundance of the gelatinase biosynthesis-activating pheromone (GBAP) (Bourgogne et al. 2006, Del Papa and Perego 2011). There are three well-studied operons that demonstrate the highest fold-change in gene expression upon initial activation by the QS regulator FsrA (Bourgogne et al. 2006, Del Papa and Perego 2011, Teixeira et al. 2013). The first of these is the *fsrBDC* QS locus, which encodes the machinery for the QS system. This includes FsrC, the transmembrane sensor-transmitter; FsrD, a precursor of GBAP; and FsrB, which processes the FsrD propeptide into GBAP (Nakayama et al. 2001, 2006, Del Papa and Perego 2011). The second operon controlled by FsrA encodes the enterocin EntV, which has activity against Gram-positive bacteria, fungi, and *Drosophila* (Teixeira et al. 2013, Dundar et al. 2015, Graham et al. 2017). The final operon regulated by the Fsr QS system contains the genes *gelE* and *sprE* (Qin et al. 2001, Teixeira et al. 2013). Enterococcal gelatinase (GelE), or gelatinase, is a secreted metalloprotease frequently associated with virulence in enterococci and is vital for initiation of biofilm formation (Garsin et al. 2001, Engelbert et al. 2004, Mohamed et al. 2004, Gaspar et al. 2009, Thomas et al. 2009). SprE is a serine protease also associated with virulence (Garsin et al. 2001, Engelbert et al. 2004, Jha et al. 2005). In addition to its roles in virulence, GelE plays a role in the postprocessing of SprE and EntV (Kawalec et al. 2005, Brown et al. 2019). Additionally, GelE and SprE have both been shown to be involved in the postprocessing of the autolysin AtlA, although the role of SprE in this context has been contested (Thomas et al. 2009, Stinemetz et al. 2017).

In this paper, we used a proteomic approach to explore the interaction between the enterococcal phage VPE25 and its *E. faecalis* host. We found time-dependent trends in phage protein production and identified correlations between gene expression and protein abundance levels during infection. Investigation of the changes in bacterial protein abundance during phage predation revealed large-scale trends in the abundance of a wide variety of proteins. We show that decreased levels of the QS-regulated protein GelE, and subsequent downstream changes in the production of the murein hydrolase modulator LrgA and antiholin-like protein LrgB, influence the outcome of phage infection.

Materials and methods

Bacterial strains, bacteriophages, and plasmids

All bacterial strains used in this study have been previously published and are detailed in Table S1 (Qin 2000, Paulsen et al. 2003, Bourgogne et al. 2008, Thomas et al. 2008, Guiton et al. 2009, Dale et al. 2015, 2018, Graham et al. 2017). Transposon mutants selected from an arrayed library were confirmed using PCR (Dale et al. 2018). Phages, plasmids, and primers used in this study are also detailed in Table S1 (Trotter and Dunny 1990, Perez-Casal et al. 1991, Duerkop et al. 2016, Chatterjee et al. 2019, Sheriff et al. 2024). *Enterococcus faecalis* strains were grown in Todd–Hewitt broth (THB) with aeration or on THB agar plates at 37°C. Complementation and empty vectors were selected in *E. faecalis* strains using 15 μg/ml chloramphenicol or 10 µg/ml tetracycline as appropriate.

RNA-seq analysis

A previously published RNA-seq dataset, generated in a parallel experiment, was reanalyzed for phage transcript abundances (EMBL-EBI ArrayExpress database, accession number E-MTAB-8546) (Parkinson et al. 2007, Chatterjee et al. 2020). RNA sequencing reads were analyzed for quality using FastQC v0.12.0 (Andrews 2010). Reads were mapped to the VPE25 open reading frames (ORFs) using Salmon v1.10.2 (Patro et al. 2017). The output read quantities, as reported in the nascent quant.sf file, were used to create relative abundance calculations by dividing the transcripts per million (TPM) for a given ORF by the total number of TPMs for a sample. ORFs were ranked by their abundance for each timepoint, and this ranking was used to inform heatmap rings in Fig. 1(A), generated using the R package Circlize (Gu et al. 2014).

Preparation of samples for proteomics

Enterococcus faecalis cultures were infected with VPE25 as described previously (Chatterjee et al. 2020). Four replicate samples of 4 ml each were taken at 0, 10, 20, and 40 min after VPE25 treatment and pelleted. Pelleted samples were resuspended in 300 µl of SDT-lysis buffer (4% (w/v) SDS, 100 mM Tris-HCl, 0.1 M DTT). Cells were lysed by bead-beating using a Bead Ruptor Elite (OMNI) with Matrix Z beads (MP Biomedicals) for two cycles of 45 s at 6 m/s. Samples were incubated at 95°C for 10 min. Tryptic digests of protein extracts were prepared following the filter-aided sample preparation (FASP) protocol described previously, with minor modifications as described in Kleiner et al. (2017) and Wiśniewski et al. (2009). Lysate was not cleared by centrifugation after boiling the sample in lysis buffer. The whole lysate was loaded onto the filter units used for the FASP procedure. Centrifugation times were reduced to 20 min as compared to Kleiner et al. (2017). Peptide concentrations were determined with the Pierce Micro BCA assay (Thermo Scientific) using an Epoch2 microplate reader (Biotek) following the manufacturer's instructions.

LC-MS/MS

All samples were analyzed by 1D-LC-MS/MS as described previously, with the modification that a 75-cm analytical column and a 140-min long gradient were used (Hinzke et al. 2019). For each sample run, 400 ng peptide were loaded with an UltiMateTM 3000 RSLCnano Liquid Chromatograph (Thermo Fisher Scientific) in loading solvent A (2% acetonitrile, 0.05% trifluoroacetic acid) onto a 5-mm, 300 µm ID C18 Acclaim® PepMap100 precolumn (Thermo Fisher Scientific). Separation of peptides on the analytical column (75 cm × 75 µm analytical EASY-Spray column packed with PepMap RSLC C18, 2 µm material, Thermo Fisher Scientific) was achieved at a flow rate of 300 nl/min using a 140-min gradient going from 95% buffer A (0.1% formic acid) to 31% buffer B (0.1% formic acid, 80% acetonitrile) in 102 min, then to 50% B in 18 min, to 99% B in 1 min, and ending with 99% B. The analytical column was heated to 60°C and was connected to a Q Exactive HF hybrid quadrupole-Orbitrap mass spectrometer (Thermo Fisher Scientific) via an Easy-Spray source. Eluting peptides were ionized via electrospray ionization. Carryover was reduced by one wash run (injection of 20 µl acetonitrile, 99% eluent B) between samples. Full scans were acquired in the Orbitrap at 60 000 resolution. The 15 most abundant precursor ions were selected for fragmentation and MS/MS scans were acquired at 15 000 resolution. The mass (m/z) 445.12003 was used as lock mass. Ions with charge state +1 were excluded from MS/MS analysis. Dynamic exclusion was set to 18 s. Roughly, 120 000 MS/MS spectra were acquired per sample.

Protein identification

A database containing protein sequences from *E. faecalis* OG1RF (NC_017316.1) and phage VPE25 (LT615366.1), both downloaded from NCBI, were used (Clark et al. 2016, O'Leary et al.

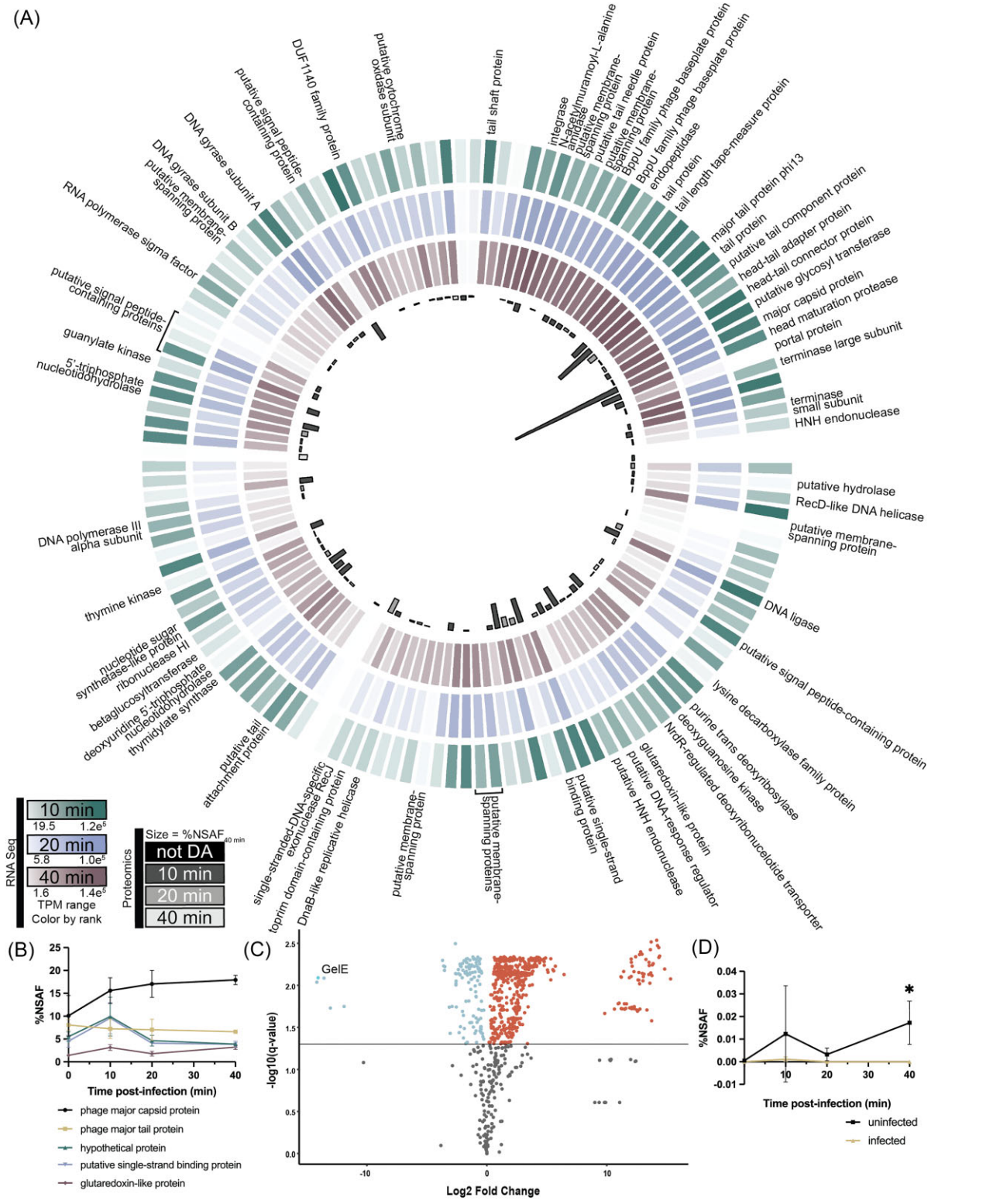

Figure 1. Phage infection of *E. faecalis* leads to diverse changes in protein expression. (A) Combined transcriptomic and proteomic data for phage VPE25. Each column represents one phage gene, with available gene annotations listed alongside corresponding columns. The outer three rings represent average TPM colored by rank at 10, 20, and 40 min postinfection. The innermost ring represents the % normalized spectral abundance factors (%NSAF) of each corresponding protein at 40 min postinfection. %NSAF abundance bars are color coded by the timepoint at which they are first identified as significantly differentially abundant (DA). (B) %NSAF values of the five most abundant phage proteins at 40 min postinfection are charted over the course of infection. Points represent an average of at least three biological replicates. Error bars represent standard deviation. (C) Volcano plot of bacterial proteins DA at 40 min postinfection between the infected and uninfected samples. Log_2-transformed fold-change between the two samples is shown on the *x*-axis. Negative log_{10}-transformed *q*-values are shown on the *y*-axis with a line at a significance cut-off of $q < 0.05$. Proteins with a *q*-value of zero were excluded. (D) %NSAF of GelE over time in both the infected and uninfected samples. Points represent an average of four biological replicates. Significance was determined using student's *t*-tests corrected for multiple hypothesis testing using a permutation-based false discovery rate of 5%. Error bars represent standard deviation. * FDR ≤ 5%.

2016). Sequences of common laboratory contaminants were included by appending the cRAP protein sequence database (http://www.thegpm.org/crap/). The final database contained 2893 protein sequences. Searches of the MS/MS spectra against this database were performed with the Sequest HT node in Proteome Discoverer version 2.2.0.388 (Thermo Fisher Scientific) as previously described (Petersen et al. 2016). Only proteins identified with medium or high confidence were retained resulting in an overall false discovery rate of <5%.

Protein quantification and statistical analyses

For quantification of bacterial proteins, normalized spectral abundance factors (NSAFs) were calculated and multiplied by 100% to obtain relative protein abundance (Zybailov et al. 2006). The NSAF values were loaded into Perseus version 1.6.2.3 and $\log_2$ transformed (Tyanova et al. 2016). Only proteins with valid values in four replicates of at least one treatment were considered for further analysis. Missing values were replaced by a constant number that was lower than any value across the experiment. Differentially abundant (DA) proteins between conditions were calculated using student's *t*-tests corrected for multiple hypothesis testing using a permutation-based false discovery rate of 5%. As the number of phage proteins is small and their relative abundances are heavily influenced by the overall abundance of the bacterial proteins in the cultures, we used a centered-log ratio (CLR) transformation for more robust analysis of compositional data (Fernandes et al. 2014). The CLR was calculated for all proteins, both phage and bacterial. CLR values for phage proteins were loaded into Perseus 1.6.2.3 where *t*-tests were performed as described above (Tyanova et al. 2016). Since the spectral counts at t0 (0 min postinfection) were much lower than the other time points, only proteins with 70% of total values across conditions with more than 20 peptide spectral matches (PSMs) were considered for comparisons with t0. For comparisons between the 10, 20, and 40 min postinfection time points, no PSM cut-off was employed. Replacement of missing values and *t*-tests were performed as described above.

Plaque assays

A volume of 1 ml of overnight bacterial culture was pelleted at 21 000 × *g* for 1 min and resuspended in 2 ml SM-plus phage buffer [100 mM NaCl, 50 mM Tris-HCl, 8 mM $MgSO_4$, and 5 mM $CaCl_2$ (pH 7.4)] (Duerkop et al. 2016). Approximately, 15 plaque-forming units (PFU) of phage were added to 120 μl of resuspended bacterial culture and incubated statically at room temperature for 5 min. Following incubation, 5 ml of molten THB top agar (0.35% agar, unless otherwise noted) supplemented with 10 mM $MgSO_4$ was added to the suspension and poured over a 1.5% THB agar plate supplemented with 10 mM $MgSO_4$. For supplementation of plates with spent media, overnight cultures of *E. faecalis* were subcultured to a starting OD_{600} of 0.025 and grown for 6 h to achieve maximum gelatinase activity. Spent media was pelleted at 4600 × *g* for 3 min, and supernatant was filtered through a 0.45-µm filter. Molten THB top agar (0.7% agar) was mixed 1:1 with filtered supernatant for a final concentration of 0.35% agar. Spent media top agar was supplemented with 10 mM $MgSO_4$, and plaque assays were performed as described above. Plates were incubated upright at 37°C for 24 h unless otherwise noted. Photos of plates were taken on an iPhone 12, and plaque diameters were measured using ImageJ v1.53t (Schneider et al. 2012). A ruler was included in each image to determine scale.

Results

Assessment of VPE25 transcript and protein abundances during *E. faecalis* infection

To understand global protein regulation and abundances during phage infection of *E. faecalis*, we infected *E. faecalis* OG1RF with the siphophage VPE25 (Duerkop et al. 2016). Mid-log cultures of *E. faecalis* were infected with VPE25 at a multiplicity of infection of 10. Samples were taken at 0, 10, 20, and 40 min postinfection and subjected to LC-MS/MS-based proteomics analyses. We compared the phage-encoded protein abundances to a previously generated RNA-Seq dataset of VPE25 infected *E. faecalis* OG1RF, where the experimental parameters were identical (Chatterjee et al. 2020). From the RNAseq, we identified 131 phage transcripts throughout infection (Table S2). Proteomic analysis identified 93 of those transcripts as proteins (Table S3).

Figure 1(A) shows the VPE25 transcript and protein abundances throughout infection. Few proteins were detected at the initiation of infection, and it is likely that those detected were either present in the virion or rapidly expressed following DNA entry. Many replication proteins, such as DNA polymerase and DNA helicases, were significantly DA after only 10 min postinfection (Table S3). By 20 min postinfection, we saw increases in abundance of additional replication machinery, such as DNA gyrase subunits A and B. Virion components, primarily proteins involved in assembly of the tail, were also DA at this time, as was the phage lysin. Final virion components, including the portal protein and the head maturation protease, were DA by 40 min postinfection. Notably, the most abundant phage protein at each timepoint was the major capsid protein, whose relative abundance continued to increase throughout the course of infection (Fig. 1B, Table S3). The major capsid transcript levels reached the top ten most abundant phage transcripts at the 10-min timepoint and remained among the most abundant transcripts throughout infection (Table S2).

A high number of detected phage transcripts and proteins were annotated as genes of unknown function. Of the 133 putative genes in the VPE25 genome, more than 60% are hypothetical. Many of these uncharacterized proteins were expressed at a level equal to or above proteins with characterized functions. For example, SCO93409.1 is an uncharacterized phage protein whose abundance at 40 min was third only to the major capsid and major tail proteins (Fig. 1B). *In silico* analysis of these hypothetical proteins failed to provide insight on their potential function, with more than half having no conserved domains identified via InterProScan (Jones et al. 2014). Together these data show that the majority of VPE25 proteins are expressed during infection, many of which are proteins of unknown function.

Enterococcus faecalis responds to VPE25 infection by altering its gene expression and protein abundances

Our understanding of bacterial gene expression levels in response to phage infection and how this corresponds to protein abundances is limited. While transcript data is often used as a stand-in for shifts in proteomic abundances, comparative analyses show that these are often not fully concordant (Weintraub et al. 2019, Wolfram-Schauerte et al. 2022). In fact, many of the most DA bacterial proteins in our analysis are relatively unchanged at the transcript level when compared to our previously published RNA-Seq dataset (Table 1, Table S4) (Chatterjee et al. 2020).

Of the 2647 genes in the *E. faecalis* OG1RF genome, 2550 were detected as transcripts (Chatterjee et al. 2020). Of those transcripts, 1225 proteins were detected using proteomics. A total of 680

Table 1. Proteins with the 20 highest and lowest differential abundance ratio (DAR) values at 40 min postinfection.

Gene name	Description	DAR40	Recovered from transposon library?
High DAR_{40} genes			
secY (*OG1RF_10171*)	Preprotein translocase subunit SecY	86.97	No, not present
OG1RF_11743	TetR/AcrR family transcriptional regulator	52.26	Yes
OG1RF_11417	Pyridoxal phosphate-dependent aminotransferase	47.66	Yes
OG1RF_10804	ATP-binding protein	45.55	Yes
OG1RF_12485	Alkaline phosphatase family protein	40.55	Yes
phoU (*OG1RF_11465*)	Phosphate signaling complex protein	40.16	Yes
OG1RF_10823	AAA family ATPase	34.49	Yes
OG1RF_11853	Homoserine dehydrogenase	33.26	Yes
yidC (*OG1RF_11837*)	Membrane protein insertase	29.87	Yes
bgsB (*OG1RF_12192*)	Glycosyltransferase family 4 protein	27.65	Yes
rsmG (*OG1RF_12545*)	16S rRNA (guanine(527)-N(7))-methyltransferase	27.43	Yes
OG1RF_11964	Mur ligase family protein	27.43	No, not present
citD (*OG1RF_12566*)	Citrate lyase acyl carrier protein	24.39	No, not present
OG1RF_11639	DUF3013 family protein	23.06	Yes
dltA (*OG1RF_12112*)	D-alanine—poly(phosphoribitol) ligase subunit	22.09	Yes
OG1RF_11645	Class I SAM-dependent methyltransferase	21.34	No, not present
OG1RF_10575	Alanine ligase	21.07	No, not present
OG1RF_12200	NAD(P)/FAD-dependent oxidoreductase	21.05	No, not present
OG1RF_12473	tRNA-dihydrouridine synthase	20.22	Yes
OG1RF_10734	RNA-binding protein	20.03	Yes
Low DAR_{40} genes			
gelE (*OG1RF_11526*)	M4 family metallopeptidase coccolysin	0.00	Yes
OG1RF_10381	Lipoate—protein ligase	0.00	Yes
OG1RF_10282	S-methyltransferase	0.00	Yes
msrA (*OG1RF_11394*)	Peptide-methionine (S)-S-oxide reductase	0.00	No, not present
OG1RF_11885	DUF2129 domain-containing protein	0.00	Yes
OG1RF_10952	CsbD family protein	0.08	No, not present
OG1RF_11211	V-type ATPase subunit	0.08	Yes
OG1RF_10532	DUF1700 domain-containing protein	0.09	Yes
OG1RF_11274	Nucleotide pyrophosphohydrolase	0.09	No, not present
OG1RF_10750	PTS sugar transporter subunit IIB	0.11	No, not present
opp2D (*OG1RF_12370*)	ABC transporter ATP-binding protein	0.12	Yes
OG1RF_10751	PTS lactose/cellobiose transporter subunit IIA	0.13	No, not present
OG1RF_11463	PspC domain-containing protein	0.16	No, not present
OG1RF_10660	AAA family ATPase	0.16	Yes
OG1RF_11909	Hypothetical protein	0.17	Yes
OG1RF_12106	MBL fold metallo-hydrolase	0.17	Yes
atpF (*OG1RF_11990*)	F0F1 ATP synthase subunit B	0.17	No, not present
OG1RF_11402	LapA family protein	0.17	No, not present
OG1RF_11033	LTA synthase family protein	0.17	No, not present
OG1RF_10795	Hypothetical protein	0.19	Yes

proteins were DA between infected and uninfected *E. faecalis* by 40 min (Fig. 1C, Table S4). There was no statistical difference in bacterial protein relative abundances at the 10-min timepoint, and at 20 min postinfection only six proteins were DA (Fig. S1A). The limited differences in protein abundances at the earlier timepoints reflect a lag time between the transcriptional response, which begins by the 10-min timepoint, and the time it takes to translate those transcripts into proteins (Chatterjee et al. 2020). All of the DA proteins at 20 min remained DA at the 40-min timepoint with the exception of OG1RF_12042, a CYTH domain-containing protein.

The differential abundance ratio (DAR) was calculated as the relative change in abundance of a protein between the infected and uninfected samples at each timepoint. The DAR at 40 min (DAR_{40}) was used to identify potential key effectors of bacteria–phage interactions during infection (Table 1). Proteins with high DAR values, such as SecY, are at an increased level during phage infection, while proteins with low DAR values, like AtpF, are found in decreased abundance during phage infection. This up- and downregulation of protein abundances can be attributed to the bacterium responding to phage infection or when phage-encoded proteins hijack bacterial host processes leading to changes in protein abundances. To determine which, if any, of these proteins may be integral to phage virulence during infection, we used mutants from an arrayed *E. faecalis* OG1RF transposon library and screened them for changes in phage infectivity (Dale et al. 2018). Mutants selected represent available transposon insertions in genes whose proteins were most over- or under-represented at 40 min as indicated by DAR (Table 1). While no differences were seen in the number of viable PFU on each strain tested (Fig. S1B), a change in plaque morphology was noted on the *gelE*-Tn mutant, a protein whose expression is undetected at 40 min (Fig. 1D).

Enterococcus faecalis gelatinase alters phage infection

VPE25 forms clear plaques with a well-defined border ~1 mm in diameter on *E. faecalis* OG1RF. However, after 24 h of plaque formation on an in-frame *gelE* deletion strain (OG1RFΔ*gelE*), VPE25 forms a central zone of clearing surrounded by a large turbid ring, which more than doubles the overall diameter (Fig. 2A). This phenotype suggests that when GelE is absent, bacterial cells are more susceptible to phage infection associated factors. This "halo" morphology is rescued through the addition of *gelE* on a constitutive expression vector (pLZ12A:: *gelE*) (Fig. 2B and C). The *gelE* gene encodes enterococcal gelatinase, a secreted protease that targets a variety of substrates and is regulated by the Fsr QS system (Mäkinen et al. 1989, Mäkinen and Mäkinen 1994, Qin et al. 2001, Waters et al. 2003, Kawalec et al. 2005, Park et al. 2007, 2008, Teixeira et al. 2013, Brown et al. 2019). GelE is one of five proteins, which were undetected in phage-infected samples by 40 min postinfection and thus has a DAR of 0, supporting our previous finding that the transcription of QS-regulated genes, including *gelE*, are significantly lower during phage infection (Table 1, Table S4) (Chatterjee et al. 2020). While the proteomics analyses were performed in infected liquid cultures, it appears that GelE is downregulated in plates as well, albeit at a slower rate. Specifically, as infection progresses in plates, plaques on OG1RF, which were previously nonhaloed begin to develop small haloes. Plaques on OG1RF and OG1RFΔ*gelE* + pLZ12A:: *gelE* phenocopy each other at 24 h; however, the overexpression of *gelE* prevents the development of these small halos and significantly limits the overall plaque diameter at the 48-h timepoint (Fig. 2C and D).

To further investigate this phenotype, we assessed phage plaque morphology on *E. faecalis* OG1RFΔ*fsrA*, a strain lacking the QS master regulator *fsrA*. Again, plaques showed a halo morphology, and plaque diameter was significantly larger than wild type (Fig. 2E). GelE cleaves the target proteins EntV and SprE, which are both under the control of FsrA, as well as AtlA, an autolysin that is involved in biofilm formation (Qin et al. 2001, Kawalec et al. 2005, Thomas et al. 2009, Dundar et al. 2015, Graham et al. 2017, Stinemetz et al. 2017, Brown et al. 2019). We tested deletion mutants of *entV*, *sprE*, and *atlA* for plaque morphology during VPE25 infection. Deletion of *entV* or *atlA* showed no change in plaque morphology or size, but a *sprE* transposon mutant strain formed haloed plaques similar to OG1RFΔ*gelE* and OG1RFΔ*fsrA* (Fig. 2F). GelE-dependent changes in the viability of extracellular virions and the ability of VPE25 phages to adsorb to *E. faecalis* cells were also tested; however, we observed no significant differences regardless of the presence or absence of GelE (Fig. S2B and C).

The top agar overlay plaque assay supports the diffusion of both phage and secreted factors, such as GelE, through the top agar. We varied the agar density to look for changes in plaque size to determine if this phenotype is associated with diffusion. Plaque assays were performed using either double (0.7% agar) or half (0.175% agar) the normal concentration of soft agar in the overlay, while all other parameters remained constant. As the agar concentration within the overlay increased, the size of VPE25 plaques and their halos on OG1RFΔ*gelE* decreased (Fig. 2G). However, when wild type OG1RF is infected with VPE25, the average plaque diameter does not change regardless of the agar concentration, suggesting that GelE diffusion is indeed responsible for this phenotype.

Because GelE is secreted and diffusible within the agar, we hypothesized that the addition of spent media from wild type OG1RF cultures could limit the development of haloed plaques on OG1RFΔ*gelE*. Spent media from cultures of OG1RF wild type or OG1RFΔ*gelE* was supplemented into plaque assays for both OG1RF and OG1RFΔ*gelE*. No significant changes in diameter were observed in plaques on OG1RF regardless of the spent media used. However, the addition of OG1RF wild type spent media significantly reduced the size of plaques on OG1RFΔ*gelE* at the 72-h timepoint (Fig. 2H). This phenotype is only significant at this late timepoint as the initial small differences in plaque diameter become more apparent as plaques continue to grow over time.

Additional *E. faecalis* strains and phages show altered infectivity that is dependent on GelE

To determine if the haloed plaque morphology was unique to *E. faecalis* OG1RF and VPE25, we tested VPE25 plaque morphology on *E. faecalis* V583, a genetically distinct vancomycin-resistant isolate (Bourgogne et al. 2008). In a *gelE* mutant of V583 (V583Δ*gelE*), VPE25 plaques develop a similar halo morphology, and the plaque diameter is significantly larger when compared to wild type cells (Fig. 3A). However, unlike OG1RFΔ*gelE*, the halo morphology is not well-observed at 24 h and is only prominent in the V583 background after 48 h (Fig. S3A). The halos observed in V583Δ*gelE* are also present in a double deletion of both *gelE* and *sprE* (V583Δ*gelE*Δ*sprE*), but not present in the *sprE* deletion alone (V583Δ*sprE*) (Fig. 3A).

To determine if this halo plaque morphology was unique to the phage VPE25, we used a panel of genetically distinct phages and measured plaque diameters on OG1RF and OG1RFΔ*gelE*. In addition to VPE25, the phage G01 produced a halo phenotype and significantly larger plaques after 48 h of infection (Fig. 3B). G01 is a 41-kb phage isolated from the Ganges River in India (Sheriff et al. 2024). While both VPE25 and G01 are siphophages with icosahedral heads and noncontractile tails, the two phages share greater than 30% nucleotide identity in only four genes as identified via clinker (Fig. S4A) (Gilchrist and Chooi 2021). Specifically, these homologous genes encode a lysin, glutaredoxin, a DUF1140 domain-containing protein, and a hypothetical protein. Interestingly, while the VPE25 and G01 lysins share 65% identity across 66% coverage, most of the homology is focused in the amidase domain (Fig. S4B) (Altschul et al. 1997). These data indicate that GelE-mediated plaque morphology is neither *E. faecalis* strain- or phage-dependent.

GelE regulation of the murein hydrolase regulator *lrgA* and antiholin-like protein *lrgB* provides protection from phage-mediated inhibition

Previous work in *E. faecalis* V583 demonstrated an upregulation of the *lrgAB* operon in the presence of *gelE* (Teixeira et al. 2013). While the function of the *lrgAB* locus is uncharacterized in *E. faecalis*, LrgA and LrgB are involved in repression of murein hydrolase activity and decreased autolysis in *Staphylococcus aureus* and their expression is dependent on the Agr QS system (Fujimoto et al. 2000, Groicher et al. 2000). We hypothesized that *lrgA* and/or *lrgB* play a role in limiting phage-mediated haloed plaque formation. The *lrgAB* locus is regulated by the LytSR two-component system, located directly upstream of its operon. LytSR is hypothesized to activate in the presence of extracellular GelE, after which it increases transcription of *lrgAB* (Teixeira et al. 2013). While the functions of *lrgA* and *lrgB* have not been studied extensively in enterococci, they have been shown to be upregulated during growth in blood (Vebø et al. 2009).

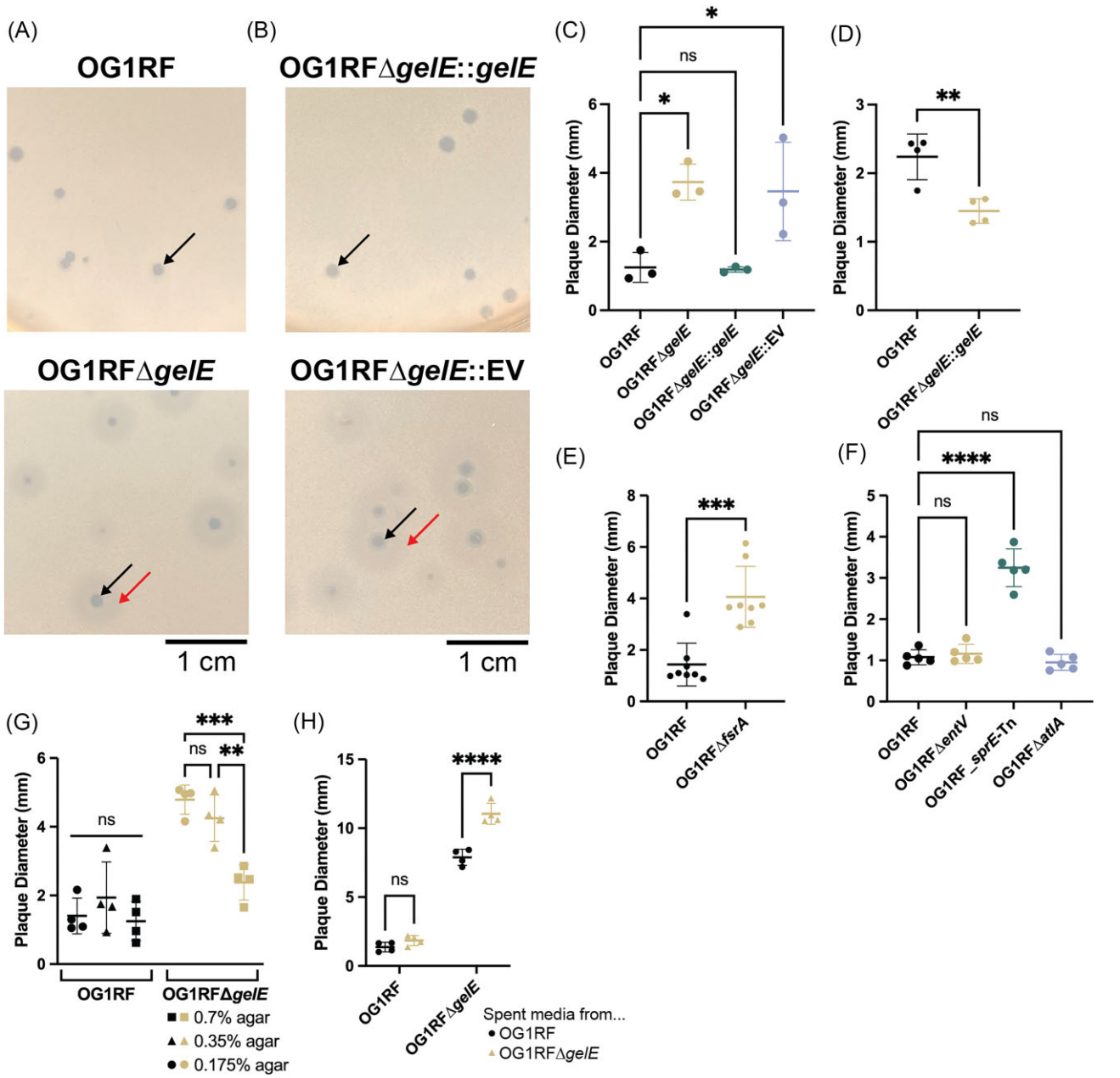

Figure 2. Phage VPE25 plaque morphology is altered in the absence of *gelE*. (A) VPE25 plaques on an *E. faecalis* OG1RF top agar overlay are small with distinct edges, while plaques on an OG1RFΔ*gelE* overlay are larger and have a halo phenotype. (B) Complementation of OG1RFΔ*gelE* with *gelE* on a plasmid (OG1RFΔ*gelE*:: *gelE*). (A and B) Clear edges of the central lytic zones of plaques are denoted with a black arrow. Where present, halo edges are denoted with a red arrow. (C) Average plaque diameters are significantly larger in OG1RFΔ*gelE* and OG1RFΔ*gelE*:: EV than in OG1RF or OG1RFΔ*gelE*:: *gelE*. Data represents average plaque diameter at 24 h from three biological replicates. (D) Plaque diameter is significantly smaller over time on the OG1RFΔ*gelE*:: *gelE* complement strain. Data represents average plaque diameter at 48 h from four biological replicates. (E) VPE25 plaques on OG1RFΔ*fsrA* are significantly larger than on OG1RF. Data represents average plaque diameter at 24 h from eight biological replicates. (F) Average plaque diameters are significantly larger than wild type in overlays of *E. faecalis sprE*-Tn when compared to OG1RF. Data represents average plaque diameter at 24 h from five biological replicates. (G) Plaque diameter on OG1RFΔ*gelE* varies with concentration of agar in top agar overlay. Data represents average plaque diameter at 24 h from four biological replicates. Significance was determined using two-way ANOVA with multiple comparisons. (H) Addition of spent media from OG1RF cultures added to top agar overlays partially abrogates the halo morphology in OG1RFΔ*gelE*. Diameter of VPE25 plaques in an OG1RFΔ*gelE* overlay is significantly smaller when OG1RF spent media is added compared to plaque diameter upon the addition of OG1RFΔ*gelE* spent media. Data represents average plaque diameter at 72 h from four biological replicates. (C, F, and H) Significance determined using one-way ANOVA with multiple comparisons. (D and E) Significance determined using unpaired *t*-test. (C, D, E, F, G, and H) Error bars represent standard deviation. **** $P \leq .0001$, *** $.0001 < P \leq .001$, ** $.001 < P \leq .01$, * $.01 < P \leq .05$, ns = not significant.

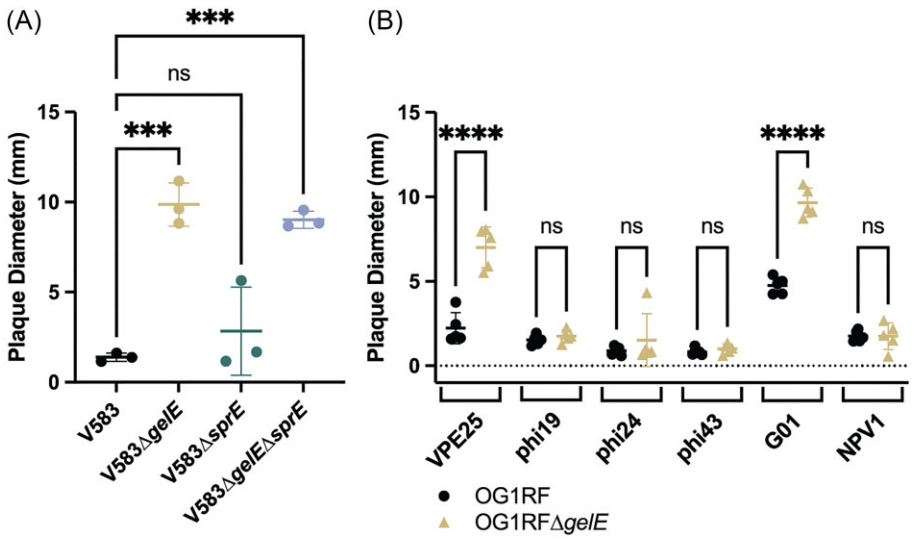

Figure 3. Distinct phages and *E. faecalis* strains are impacted by the presence of GelE. (A) Average plaque diameter on V583Δ*gelE* and V583Δ*gelE*Δ*sprE* is significantly larger than wild type V583. Data represents average plaque diameter at 48 h from three biological replicates. Significance was determined using one-way ANOVA with multiple comparisons. (B) The plaque diameter of VPE25 and G01 plaques is significantly larger on an overlay of OG1RFΔ*gelE* when compared to OG1RF. Data represents average plaque diameter at 48 h from five biological replicates. Significance determined using two-way ANOVA with multiple comparisons. (A and B) Error bars represent standard deviation. **** $P \leq .0001$, *** $.0001 < P \leq .001$, ns = not significant.

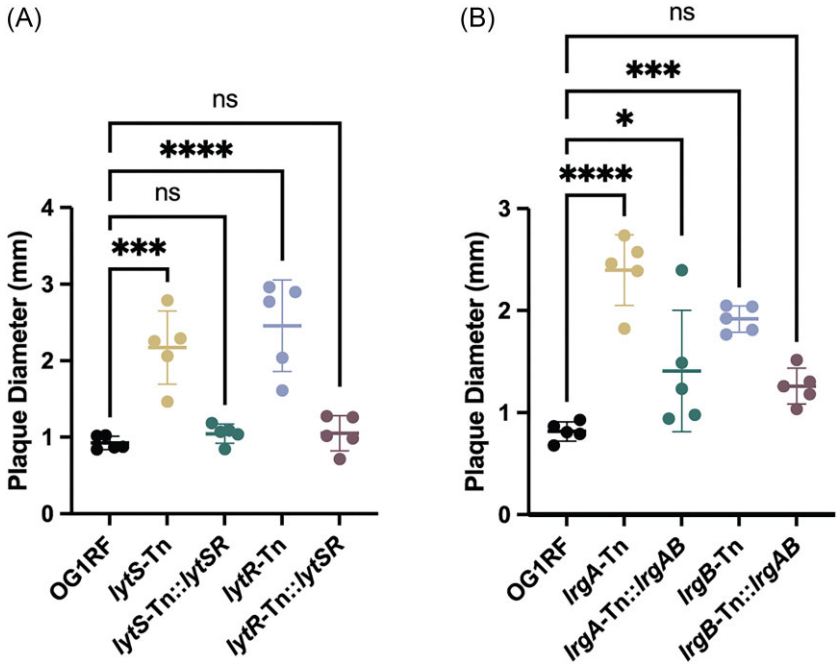

Figure 4. Mutation of *lrgA* and *lrgB* genes results in altered plaque morphology. (A) Average plaque diameter on *E. faecalis lytS*-Tn and *lytR*-Tn mutants is significantly larger than on OG1RF or complemented strains. (B) Average plaque diameter on *lrgA*-Tn and *lrgB*-Tn mutants is significantly larger than on wild type or complemented strains. (A and B) Data represents average plaque diameter at 24 h from five biological replicates. Significance determined using one-way ANOVA with multiple comparisons. Error bars represent standard deviation. **** $P \leq .0001$, *** $.0001 < P \leq .001$, * $.01 < P \leq .05$, ns = not significant.

Considering the role of LrgA and LrgB in limiting murein hydrolase activity, we hypothesized that they may be involved in protection against phage-mediated extracellular lysis. VPE25 plaque diameters on *lytS*-Tn and *lytR*-Tn mutants were significantly larger than wild type (Fig. 4A). Next, the plaque assay was repeated with *lrgA*-Tn and *lrgB*-Tn mutants, showing that plaque diameters are significantly larger than wild type OG1RF (Fig. 4B). Complementation of these genes restores plaque diameters to that of wild type OG1RF (Fig. 4A and B). Together, our data suggest that the murein hydrolase regulator LrgA and the antiholin LrgB are ultimately responsible for the altered plaque morphology in the absence of GelE and support the notion that this activity is mediated first by GelE and then by the LytSR two-component system. The underabundance of proteins like GelE during phage infection may be due in part to phage-mediated changes in enterococcal QS to facilitate an environment more permissible to phage infection. This is further supported by the increased phage-dependent inhibition seen on plates in the absence of these genes.

Discussion

The continued rise in antibiotic resistant bacterial infections has led to renewed interest in alternative antimicrobials, including phages. However, gaps in our understanding of phage biology and infection dynamics limit the full potential of emerging phage therapeutics. In this study, we used proteomics to probe the complexities of phage infection and understand the interplay between phages and *E. faecalis*. The resulting dataset provided insights into the timing of phage protein expression during infection, as well as identifying altered abundances of hundreds of bacterial proteins during infection, primarily those involved in cell wall remodeling and bacterial metabolism. Additionally, this work revealed a role for the FsrA-regulated protease GelE, and to a lesser extent the protease SprE, in driving phenotypic changes in phage plaque morphology. This phenotypic change is due to ablated activity of the murein hydrolase regulator LrgA and the antiholin LrgB, which we hypothesize aid in protection from increased phage-mediated attack (Fig. 5). Future development of phages for clinical application may exploit this phenotype to allow for phage modulation of the virulence factor GelE to reduce *E. faecalis* virulence.

GelE was investigated because it is significantly underabundant during phage infection (Fig. 1C and D, Table 1, Table S4). Because GelE is a secreted protein, our methodology may have limited its detection. However, the observation that GelE is significantly underabundant during phage infection is consistent with the repression of QS-regulated transcripts during phage infection of *E. faecalis*, including *gelE* and *sprE* (Chatterjee et al. 2020). Gelatinase has been previously characterized as a virulence factor and has a role in the formation of biofilms, which are well-penetrated by phages (Mohamed et al. 2004, Thomas et al. 2009, Khalifa et al. 2015, Melo et al. 2016, Morris et al. 2019). These data suggest that, in addition to aiding in the dispersal of biofilms, phages can limit biofilm initiation through repression of *gelE*. Further research may elucidate phage factors responsible for mediating the repression of enterococcal QS during infection. Inclusion of an identified gene or genes in a therapeutic phage may aid treatment by repressing the expression of Fsr-regulated virulence factors (Kawalec et al. 2005, Park et al. 2007, Del Papa and Perego 2011). GelE is secreted and thus cells, which do not produce GelE can take advantage of the gelatinase produced by neighboring bacteria as cheaters (Thomas et al. 2009, Teixeira et al. 2012). However, the supplementation of extracellular gelatinase is not sufficient to fully eliminate the halo plaque phenotype, suggesting partial abrogation of gelatinase activity may still be therapeutically beneficial (Fig. 2H).

While the absence of *gelE* is associated with the development of haloed plaques in both *E. faecalis* OG1RF and V583, deletion of *sprE* results in changes to plaque morphology only in OG1RF (Fig. 2C, F, and 3A). These strains share 98.82% and 99.30% amino acid identity across the full sequences of GelE and SprE, respectively (Altschul et al. 1997). With such high similarity and a well-characterized role for GelE in the postprocessing of SprE, it remains unclear why interruption of *sprE* does not result in haloed plaques in V583 (Kawalec et al. 2005). It is possible that SprE, in addition to GelE, is required for processing a downstream factor, which is processed by GelE alone in V583, or in conjunction with an alternative protease. Postprocessing by GelE is known to impact the localization of the autolysin AtlA on the cell surface (Stinemetz et al. 2017). Bacteria often acquire phage resistance through mutations that result in changes to the structure of cell wall-associated molecules (Duerkop et al. 2016, Chatterjee et al. 2019). While the haloed plaques reported here are not dependent on AtlA, characterization of additional changes to the cell surface in the absence of *gelE*, *sprE*, or both may provide insight into the mechanism of this phenotype (Fig. 2F).

Interruption of *lrgA* and *lrgB*, which are positively regulated in the presence of GelE, also resulted in the haloed plaque morphology (Fig. 4B) (Teixeira et al. 2013). It is it unlikely that LrgA and LrgB are directly involved in the adsorption or phage DNA entry process. VPE25 infection is a two-step process. First, VPE25 adsorbs to *E. faecalis* by interacting with the enterococcal polysaccharide antigen (EPA) (Chatterjee et al. 2019). Mutation of *epa* genes results in a significant adsorption deficiency and a lack of productive infection (Chatterjee et al. 2020). Following EPA engagement, VPE25 then requires interaction with the integral membrane protein PIP_{EF} to facilitate DNA entry (Duerkop et al. 2016). In the absence of PIP_{EF}, VPE25 virions can adsorb to the *E. faecalis* cell surface but fail to eject their genomes into the host cytoplasm. LrgA and LrgB are known to repress murein hydrolase activity and autolysis in *S. aureus*, suggesting a potential role for these proteins in limiting phage-mediated extracellular lysis (Groicher et al. 2000). Further elucidating the mechanism of LrgAB-conferred protection will inform our understanding of how these proteins function during phage infection of *E. faecalis*. The similarity between the amidase domains of the G01 and VPE25 lysins, as well as the role of LrgA and LrgB in the repression of murein hydrolase activity, suggests that LrgA and LrgB may provide protection against extracellular phage lysis or "lysis from without" (Fig. 4B, Fig. S4B) (Abedon 2011).

Similar haloed plaque morphologies have been associated with the presence of phage depolymerases (Wu et al. 2019, Vukotic et al. 2020). These phage-encoded proteins can degrade a variety of bacterial polysaccharides, including capsular, extracellular, and lipopolysaccharides (Leiman et al. 2007, Cornelissen et al. 2012, Olszak et al. 2017). Although phage depolymerases have been previously associated with similar plaque phenotypes, analysis using InterProScan did not reveal any Pfam matches for such depolymerases within the genomes of phages VPE25 or G01 (Jones et al. 2014). While the mechanism of GelE-conferred protection from phage-mediated inhibition is still unknown, phages which are able to modulate the production of virulence factors such as GelE should be considered for their potential role in future therapeutic applications. Taken together, our work here provides an understanding of phage infection at the protein level and demonstrates a protective role for GelE, LrgA, and LrgB during phage infection (Fig. 5).

Acknowledgments

All LC-MS/MS measurements were made in the Molecular Education, Technology, and Research Innovation Centre (METRIC) at NC State University. The authors would like to thank Dr Julia Willett, Dr Kimberly Kline, and Dr Danielle Garsin for providing bacterial strains used in this work.

Supplementary data

Supplementary data is available at *FEMSMC Journal* online.

Conflict of interest: None declared.

Funding

This work was supported by the National Institutes of Health grants R01AI141479 (B.A.D.) and R35GM138362 (M.K.).

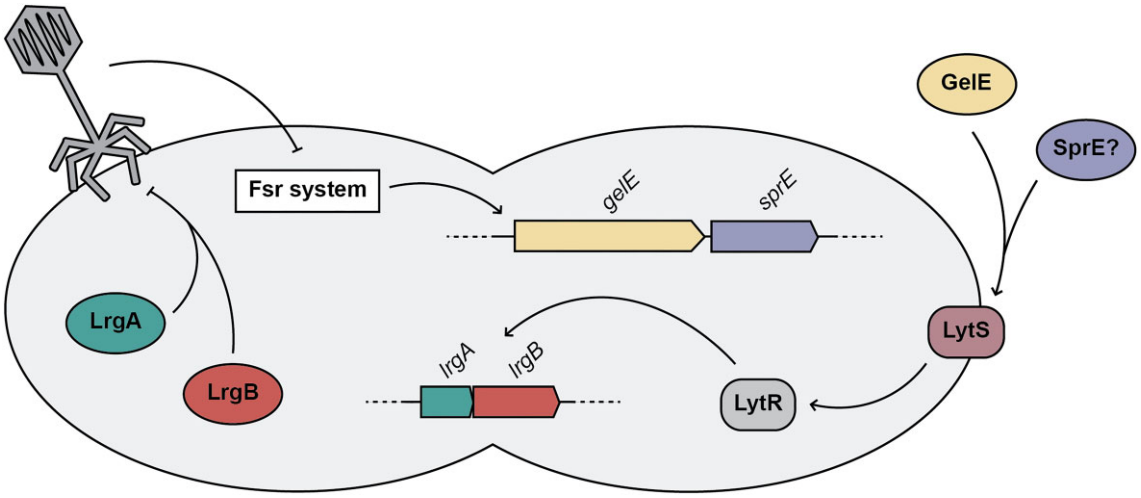

Figure 5. Enterococcal quorum-controlled proteases alter phage infection. Model figure summarizing the interactions between the Fsr QS system, GelE, SprE, LytS, LytR, LrgA, LrgB, and phage VPE25 during infection of *E. faecalis*.

Data availability

The proteomic data (MS raw files and search results) and the protein sequence database have been deposited to the ProteomeXchange Consortium via the PRIDE partner repository with the dataset identifier PXD026873 (Vizcaíno et al. 2016).

References

Abedon ST. Lysis from without. *Bacteriophage* 2011;**1**:46–49.

Agudelo Higuita NI, Huycke MM. Enterococcal disease, epidemiology, and implications for treatment. In: Gilmore MS, Clewell DB, Ike Y, Shankar N (eds), *Enterococci: From Commensals to Leading Causes of Drug Resistant Infection*.Boston: Massachusetts Eye and Ear Infirmary, 2014.

Ali L, Goraya MU, Arafat Y *et al.* Molecular mechanism of quorum-sensing in *Enterococcus faecalis*: its role in virulence and therapeutic approaches. *Int J Mol Sci* 2017;**18**:960.

Altschul SF, Madden TL, Schäffer AA *et al.* Gapped BLAST and PSI-BLAST: a new generation of protein database search programs. *Nucleic Acids Res* 1997;**25**:3389–402.

Andrews S. FastQC: a quality control tool for high throughput sequence data. Cambridge: Babraham Bioinformatics, 2010. https://www.bioinformatics.babraham.ac.uk/projects/fastqc/ (1 November 2022, date last accessed).

Bourgogne A, Garsin DA, Qin X *et al.* Large scale variation in *Enterococcus faecalis* illustrated by the genome analysis of strain OG1RF. *Genome Biol* 2008;**9**:R110.

Bourgogne A, Hilsenbeck SG, Dunny GM *et al.* Comparison of OG1RF and an isogenic *fsrB* deletion mutant by transcriptional analysis: the Fsr system of *Enterococcus faecalis* is more than the activator of gelatinase and serine protease. *J Bacteriol* 2006;**188**:2875–84.

Brown AO, Graham CE, Cruz MR *et al.* Antifungal activity of the *Enterococcus faecalis* peptide EntV requires protease cleavage and disulfide bond formation. *mBio* 2019;**10**:e01334–19.

Chatterjee A, Johnson CN, Luong P *et al.* Bacteriophage resistance alters antibiotic-mediated intestinal expansion of enterococci. *Infect Immun* 2019;**87**:e00085–19.

Chatterjee A, Willett JLE, Nguyen UT *et al.* Parallel genomics uncover novel enterococcal-bacteriophage interactions. *mBio* 2020;**11**:e03120–19.

Clark K, Karsch-Mizrachi I, Lipman DJ *et al.* GenBank. *Nucleic Acids Res* 2016;**44**:D67–72.

Cornelissen A, Ceyssens PJ, Krylov VN *et al.* Identification of EPS-degrading activity within the tail spikes of the novel *Pseudomonas putida* phage AF. *Virology* 2012;**434**:251–6.

Dale JL, Beckman KB, Willett JLE *et al.* Comprehensive functional analysis of the *Enterococcus faecalis* core genome using an ordered, sequence-defined collection of insertional mutations in strain OG1RF. *mSystems* 2018;**3**:e00062–18.

Dale JL, Cagnazzo J, Phan CQ *et al.* Multiple roles for *Enterococcus faecalis* glycosyltransferases in biofilm-associated antibiotic resistance, cell envelope integrity, and conjugative transfer. *Antimicrob Agents Chemother* 2015;**59**:4094–105.

Datta I, Sau S, Sil AK *et al.* The bacteriophage λ DNA replication protein P inhibits the *oriC* DNA- and ATP-binding functions of the DNA replication initiator protein DnaA of *Escherichia coli*. *J Biochem Mol Biol* 2005;**38**:97–103.

Del Papa MF, Perego M. *Enterococcus faecalis* virulence regulator FsrA binding to target promoters. *J Bacteriol* 2011;**193**:1527–32.

De Smet J, Zimmermann M, Kogadeeva M *et al.* High coverage metabolomics analysis reveals phage-specific alterations to *Pseudomonas aeruginosa* physiology during infection. *ISME J* 2016;**10**:1823–35.

D'Herelle F. Sur un microbe invisible antagoniste des bacilles dysentériques. *C R Acad Sci Paris* 1917;**165**:373–5.

Duerkop BA, Huo W, Bhardwaj P *et al.* Molecular basis for lytic bacteriophage resistance in enterococci. *mBio* 2016;**7**:e01304–16.

Dundar H, Brede DA, La Rosa SL *et al.* The *fsr* quorum-sensing system and cognate gelatinase orchestrate the expression and processing of proprotein EF_1097 into the mature antimicrobial peptide enterocin O16. *J Bacteriol* 2015;**197**:2112–21.

Eckburg PB, Bik EM, Bernstein CN *et al.* Diversity of the human intestinal microbial flora. *Science* 2005;**308**:1635–8.

Engelbert M, Mylonakis E, Ausubel FM *et al.* Contribution of gelatinase, serine protease, and *fsr* to the pathogenesis of *Enterococcus faecalis* endophthalmitis. *Infect Immun* 2004;**72**:3628–33.

Fernandes AD, Reid JN, Macklaim JM *et al.* Unifying the analysis of high-throughput sequencing datasets: characterizing RNA-seq, 16S rRNA gene sequencing and selective growth experiments by compositional data analysis. *Microbiome* 2014;**2**:15.

Fujimoto DF, Brunskill EW, Bayles KW. Analysis of genetic elements controlling *Staphylococcus aureus lrgAB* expression: potential role of DNA topology in SarA regulation. *J Bacteriol* 2000;**182**:4822–8.

García-Solache M, Rice LB. The enterococcus: a model of adaptability to its environment. *Clin Microbiol Rev* 2019;**32**:e00058–18.

Garsin DA, Sifri CD, Mylonakis E *et al.* A simple model host for identifying gram-positive virulence factors. *Proc Natl Acad Sci USA* 2001;**98**:10892–7.

Gaspar F, Teixeira N, Rigottier-Gois L *et al.* Virulence of *Enterococcus faecalis* dairy strains in an insect model: the role of *fsrB* and *gelE*. *Microbiology* 2009;**155**:3564–71.

Giacometti A, Cirioni O, Schimizzi AM *et al.* Epidemiology and microbiology of surgical wound infections. *J Clin Microbiol* 2000;**38**:918–22.

Gilchrist CLM, Chooi Y-H. clinker & clustermap.Js: automatic generation of gene cluster comparison figures. *Bioinformatics* 2021;**37**:2473–5.

Graham CE, Cruz MR, Garsin DA *et al.* *Enterococcus faecalis* bacteriocin EntV inhibits hyphal morphogenesis, biofilm formation, and virulence of *Candida albicans*. *Proc Natl Acad Sci USA* 2017;**114**:4507–12.

Groicher KH, Firek BA, Fujimoto DF *et al.* The *Staphylococcus aureus lrgAB* operon modulates murein hydrolase activity and penicillin tolerance. *J Bacteriol* 2000;**182**:1794–801.

Gu Z, Gu L, Eils R *et al.* Circlize implements and enhances circular visualization in R. *Bioinformatics* 2014;**30**:2811–2.

Guiton PS, Hung CS, Kline KA *et al.* Contribution of autolysin and sortase A during *Enterococcus faecalis* DNA-dependent biofilm development. *Infect Immun* 2009;**77**:3626–38.

Hatfull GF, Hendrix RW. Bacteriophages and their genomes. *Curr Opin Virol* 2011;**1**:298–303.

Hayashi H, Takahashi R, Nishi T *et al.* Molecular analysis of jejunal, ileal, caecal and recto-sigmoidal human colonic microbiota using 16S rRNA gene libraries and terminal restriction fragment length polymorphism. *J Med Microbiol* 2005;**54**:1093–101.

Hinzke T, Kouris A, Hughes RA *et al.* More is not always better: evaluation of 1D and 2D-LC-MS/MS methods for metaproteomics. *Front Microbiol* 2019;**10**:238.

Holland TL, Baddour LM, Bayer AS *et al.* Infective endocarditis. *Nat Rev Dis Primers* 2016;**2**:16059.

Huycke MM, Sahm DF, Gilmore MS. Multiple-drug resistant enterococci: the nature of the problem and an agenda for the future. *Emerg Infect Dis* 1998;**4**:239–49.

Jha AK, Bais HP, Vivanco JM. *Enterococcus faecalis* mammalian virulence-related factors exhibit potent pathogenicity in the *Arabidopsis thaliana* plant model. *Infect Immun* 2005;**73**:464–75.

Jones P, Binns D, Chang H-Y *et al.* InterProScan 5: genome-scale protein function classification. *Bioinformatics* 2014;**30**:1236–40.

Kawalec M, Potempa J, Moon JL *et al.* Molecular diversity of a putative virulence factor: purification and characterization of isoforms of an extracellular serine glutamyl endopeptidase of *Enterococcus faecalis* with different enzymatic activities. *J Bacteriol* 2005;**187**:266–75.

Khalifa L, Brosh Y, Gelman D *et al.* Targeting *Enterococcus faecalis* biofilms with phage therapy. *Appl Environ Microbiol* 2015;**81**:2696–705.

Kleiner M, Thorson E, Sharp CE *et al.* Assessing species biomass contributions in microbial communities via metaproteomics. *Nat Commun* 2017;**8**:1558.

Lake JG, Weiner LM, Milstone AM *et al.* Pathogen distribution and antimicrobial resistance among pediatric healthcare-associated infections reported to the National Healthcare Safety Network, 2011-2014. *Infect Control Hosp Epidemiol* 2018;**39**:1–11.

Leiman PG, Battisti AJ, Bowman VD *et al.* The structures of bacteriophages K1E and K1-5 explain processive degradation of polysaccharide capsules and evolution of new host specificities. *J Mol Biol* 2007;**371**:836–49.

Mäkinen PL, Clewell DB, An F *et al.* Purification and substrate specificity of a strongly hydrophobic extracellular metalloendopeptidase ("gelatinase") from *Streptococcus faecalis* (strain 0G1-10). *J Biol Chem* 1989;**264**:3325–34.

Mäkinen PL, Mäkinen KK. The *Enterococcus faecalis* extracellular metalloendopeptidase (EC 3.4.24.30; coccolysin) inactivates human endothelin at bonds involving hydrophobic amino acid residues. *Biochem Biophys Res Commun* 1994;**200**:981–5.

Melo LD, Veiga P, Cerca N *et al.* Development of a phage cocktail to control *Proteus mirabilis* catheter-associated urinary tract infections. *Front Microbiol* 2016;**7**:1024.

Mohamed JA, Huang W, Nallapareddy SR *et al.* Influence of origin of isolates, especially endocarditis isolates, and various genes on biofilm formation by *Enterococcus faecalis*. *Infect Immun* 2004;**72**:3658–63.

Morris J, Kelly N, Elliott L *et al.* Evaluation of bacteriophage antibiofilm activity for potential control of orthopedic implant-related infections caused by *Staphylococcus aureus*. *Surg Infect* 2019;**20**:16–24.

Murray CJL, Ikuta KS, Sharara F *et al.* Global burden of bacterial antimicrobial resistance in 2019: a systematic analysis. *Lancet North Am Ed* 2022;**399**:629–55.

Nakayama J, Cao Y, Horii T *et al.* Gelatinase biosynthesis-activating pheromone: a peptide lactone that mediates a quorum sensing in *Enterococcus faecalis*. *Mol Microbiol* 2001;**41**:145–54.

Nakayama J, Chen S, Oyama N *et al.* Revised model for *Enterococcus faecalis fsr* quorum-sensing system: the small open reading frame *fsrD* encodes the gelatinase biosynthesis-activating pheromone propeptide corresponding to staphylococcal AgrD. *J Bacteriol* 2006;**188**:8321–6.

O'Leary NA, Wright MW, Brister JR *et al.* Reference sequence (RefSeq) database at NCBI: current status, taxonomic expansion, and functional annotation. *Nucleic Acids Res* 2016;**44**:D733–45.

Olszak T, Shneider MM, Latka A *et al.* The O-specific polysaccharide lyase from the phage LKA1 tailspike reduces *Pseudomonas* virulence. *Sci Rep* 2017;**7**:16302.

O'Neill J. *Tackling Drug-Resistant Infections Globally: Final Report and Recommendations*. London: Wellcome Trust, 2016.

Østergaard L, Voldstedlun M, Bruun NE *et al.* Temporal changes, patient characteristics, and mortality, according to microbiological cause of infective endocarditis: a nationwide study. *JAHA* 2022;**11**:e025801.

Park SY, Kim KM, Lee JH *et al.* Extracellular gelatinase of *Enterococcus faecalis* destroys a defense system in insect hemolymph and human serum. *Infect Immun* 2007;**75**:1861–9.

Park SY, Shin YP, Kim CH *et al.* Immune evasion of *Enterococcus faecalis* by an extracellular gelatinase that cleaves C3 and iC3b. *J Immunol* 2008;**181**:6328–36.

Parkinson H, Kapushesky M, Shojatalab M *et al.* ArrayExpress—a public database of microarray experiments and gene expression profiles. *Nucleic Acids Res* 2007;**35**:D747–50.

Patro R, Duggal G, Love MI *et al.* Salmon provides fast and bias-aware quantification of transcript expression. *Nat Methods* 2017;**14**:417–9.

Paulsen IT, Banerjei L, Myers GS *et al.* Role of mobile DNA in the evolution of vancomycin-resistant *Enterococcus faecalis*. *Science* 2003;**299**:2071–4.

Perez-Casal J, Caparon MG, Scott JR *et al.* Trans-acting positive regulator of the M protein gene of *Streptococcus pyogenes* with similarity to the receptor proteins of two-component regulatory systems. *J Bacteriol* 1991;**173**:2617–24.

Petersen JM, Kemper A, Gruber-Vodicka H *et al.* Chemosynthetic symbionts of marine invertebrate animals are capable of nitrogen fixation. *Nat Microbiol* 2016;**2**:16195.

Qin X, Singh KV, Weinstock GM *et al.* Characterization of *fsr*, a regulator controlling expression of gelatinase and serine protease in *Enterococcus faecalis* OG1RF. *J Bacteriol* 2001;**183**:3372–82.

Qin X. Identification and characterization of virulence in *Enterococcus faecalis*. Thesis, Graduate School of Biomedical Sciences, University of Texas, 2000.

Rice LB, Desbonnet C, Tait-Kamradt A *et al.* Structural and regulatory changes in PBP4 trigger decreased β-lactam susceptibility in *Enterococcus faecalis*. *mBio* 2018;**9**:e00361–18.

Rossmann FS, Racek T, Wobser D *et al.* Phage-mediated dispersal of biofilm and distribution of bacterial virulence genes is induced by quorum sensing. *PLoS Pathog* 2015;**11**:e1004653.

Schneider CA, Rasband WS, Eliceiri KW. NIH image to ImageJ: 25 years of image analysis. *Nat Methods* 2012;**9**:671–5.

Schroven K, Putzeys L, Swinnen AL *et al.* The phage-encoded protein PIT2 impacts *Pseudomonas aeruginosa* quorum sensing by direct interaction with LasR. *iScience* 2023;**26**:107745.

Schwartzkopf CM, Taylor VL, Groleau MC *et al.* Inhibition of PQS signaling by the Pf bacteriophage protein PfsE enhances viral replication in *Pseudomonas aeruginosa*. *Mol Microbiol* 2024;**121**:116–28.

Sergueev K, Court D, Reaves L *et al. E. coli* cell-cycle regulation by bacteriophage lambda. *J Mol Biol* 2002;**324**:297–307.

Sghir A, Gramet G, Suau A *et al.* Quantification of bacterial groups within human fecal flora by oligonucleotide probe hybridization. *Appl Environ Microbiol* 2000;**66**:2263–6.

Sheriff EK, Andersen SE, Chatterjee A *et al.* Complete genome sequence of enterococcal phage G01. *Microbiol Resour Announc* 2024;**13**:e0121723.

Stinemetz EK, Gao P, Pinkston KL *et al.* Processing of the major autolysin of *E. faecalis*, AtlA, by the zinc-metalloprotease, GelE, impacts AtlA septal localization and cell separation. *PLoS One* 2017;**12**:e0186706.

Teixeira N, Santos S, Marujo P *et al.* The incongruent gelatinase genotype and phenotype in *Enterococcus faecalis* are due to shutting off the ability to respond to the gelatinase biosynthesis-activating pheromone (GBAP) quorum-sensing signal. *Microbiology* 2012;**158**:519–28.

Teixeira N, Varahan S, Gorman MJ *et al. Drosophila* host model reveals new *Enterococcus faecalis* quorum-sensing associated virulence factors. *PLoS One* 2013;**8**:e64740.

Thomas VC, Hiromasa Y, Harms N *et al.* A fratricidal mechanism is responsible for eDNA release and contributes to biofilm development of *Enterococcus faecalis*. *Mol Microbiol* 2009;**72**:1022–36.

Thomas VC, Thurlow LR, Boyle D *et al.* Regulation of autolysis-dependent extracellular DNA release by *Enterococcus faecalis* extracellular proteases influences biofilm development. *J Bacteriol* 2008;**190**:5690–8.

Trotter KM, Dunny GM. Mutants of *Enterococcus faecalis* deficient as recipients in mating with donors carrying pheromone-inducible plasmids. *Plasmid* 1990;**24**:57–67.

Twort FW. An investigation on the nature of ultra-microscopic viruses. *Lancet North Am Ed* 1915;**186**:1241–3.

Tyanova S, Temu T, Sinitcyn P *et al.* The Perseus computational platform for comprehensive analysis of (prote)omics data. *Nat Methods* 2016;**13**:731–40.

Tyson GH, Sabo JL, Hoffmann M *et al.* Novel linezolid resistance plasmids in *Enterococcus* from food animals in the USA. *J Antimicrob Chemother* 2018;**73**:3254–8.

Van Tyne D, Gilmore MS. Friend turned foe: evolution of enterococcal virulence and antibiotic resistance. *Annu Rev Microbiol* 2014;**68**:337–56.

Vebø HC, Snipen L, Nes IF *et al.* The transcriptome of the nosocomial pathogen *Enterococcus faecalis* V583 reveals adaptive responses to growth in blood. *PLoS One* 2009;**4**:e7660.

Vizcaíno JA, Csordas A, del-Toro N *et al.* 2016 update of the PRIDE database and its related tools. *Nucleic Acids Res* 2016;**44**:D447–56.

Vogkou CT, Vlachogiannis NI, Palaiodimos L *et al.* The causative agents in infective endocarditis: a systematic review comprising 33,214 cases. *Eur J Clin Microbiol Infect Dis* 2016;**35**:1227–45.

Vukotic G, Obradovic M, Novovic K *et al.* Characterization, antibiofilm, and depolymerizing activity of two phages active on carbapenem-resistant *Acinetobacter baumannii*. *Front Med* 2020;**7**:426.

Waters CM, Antiporta MH, Murray BE *et al.* Role of the *Enterococcus faecalis* GelE protease in determination of cellular chain length, supernatant pheromone levels, and degradation of fibrin and misfolded surface proteins. *J Bacteriol* 2003;**185**:3613–23.

Weintraub ST, Mohd Redzuan NH, Barton MK *et al.* Global proteomic profiling of *Salmonella* infection by a giant phage. *J Virol* 2019;**93**:e01833–18.

Wigington CH, Sonderegger D, Brussaard CP *et al.* Re-examination of the relationship between marine virus and microbial cell abundances. *Nat Microbiol* 2016;**1**:15024.

Williamson KE, Fuhrmann JJ, Wommack KE *et al.* Viruses in soil ecosystems: an unknown quantity within an unexplored territory. *Annu Rev Virol* 2017;**4**:201–19.

Wiśniewski JR, Zougman A, Nagaraj N *et al.* Universal sample preparation method for proteome analysis. *Nat Methods* 2009;**6**:359–62.

Wolfram-Schauerte M, Pozhydaieva N, Viering M *et al.* Integrated omics reveal time-resolved insights into T4 phage infection of *E. coli* on proteome and transcriptome levels. *Viruses* 2022;**14**:2502.

Wu Y, Wang R, Xu M *et al.* A novel polysaccharide depolymerase encoded by the phage SH-KP152226 confers specific activity against multidrug-resistant *Klebsiella pneumoniae* via biofilm degradation. *Front Microbiol* 2019;**10**:2768.

Yang J, Bowring JZ, Krusche J *et al.* Cross-species communication via *agr* controls phage susceptibility in *Staphylococcus aureus*. *Cell Rep* 2023;**42**:113154.

Zybailov B, Mosley AL, Sardiu ME *et al.* Statistical analysis of membrane proteome expression changes in *Saccharomyces cerevisiae*. *J Proteome Res* 2006;**5**:2339–47.

Received 5 May 2024; **revised** 21 June 2024; **accepted** 25 July 2024